Electronic and Sensing Properties of ZnO Nanoribbons: a DFT Analysis

M. Kovalenko, O. Bovgyra, D. Malanchuk
Ivan Franko National University of Lviv, 8, Kyrylo and Mefodiy, 79005 Lviv, Ukraine
e-mail: mariya.kovalenko@lnu.edu.ua

Introduction

Gas sensing technologies are attracting increasing attention in industry and academic research due to their widespread use in industrial manufacturing, automotive, medicine, indoor air quality control, and environmental monitoring. The increased demand for susceptible, selective, low-cost, low-power, reliable, stable, and portable sensors has stimulated extensive research into developing new sensor materials. Semiconducting metal oxides have long been considered promising candidates for gas-sensing applications due to their high sensitivity, simple fabrication methods, low cost, and high compatibility with other parts and processes. As is known, when the structural dimensions are reduced to a few nanometers, the surface-to-volume ratio increases tremendously; therefore, a large active area for interaction with the gas is provided. Zinc oxide (ZnO) is an n-type semiconductor with a wide bandgap (3.37 eV at 0 K) due to its unique optical and electronic properties, besides attracting considerable attention for potential applications such as solar cells, optoelectronic devices, nanogenerators, and catalysts, is one of the most studied sensitive materials for gas sensors. Due to their high sensitivity, stability, and low-cost advantages, ZnO nanostructures are widely used to detect gases. The synergistic combination of excellent sensing characteristics of ZnO with the potential of 1D nanostructures leads to high detection efficiency, reduced operating temperature, fast response and recovery, and improved selectivity. Therefore, in this work, we presented the study of the electronic and sensor properties of ZnO nanoribbons (ZnONRs) with armchair and zigzag edges within the density functional theory (DFT) under the adsorption of various gases (CO, CO_2, NO, NO_2).

Models and Methods

The geometry optimization of the structure ZnO nanoribbons with width n = 8 with different edges, armchair (8a-ZnONR), and zigzag (8z-ZnONR), and the study of the electronic and sensor properties of ZnONRs were carried out within DFT. ZnONR configurations with hydrogen edge passivation were also considered. The exchange-correlation potential is described using the GGA(PBE) approximation. To evaluate the weak intermolecular interaction during gas adsorption, a semi-empirical dispersion correction for van der Waals' interaction with DFT was used according to the scheme proposed by Grimm. The Hubbard corrections method to the GGA approximation, so-called the DFT+U method, was used to describe the structural and electronic properties more accurately.

Results and discussion

Fig.1 presents the structures of ZnO nanoribbons with n = 8 with different edges: armchair-like (8a-ZnONR) and zigzag-like (8z-ZnONR) after optimization. We also considered nanoribbons without passivation by hydrogen atoms (Fig. 1 a, c) and with edges passivated by H atoms (Fig. 1 b, d). For unpassivated armchair ZnO nanoribbons, significant deformation of the Zn–O bond is observed: zinc atoms shift toward the nanoribbon, while O atoms shift in the opposite direction, and the bond length of the edge Zn–O atoms decreases from 1.92 Å for the nonoptimized NR to 1.81–1.76 Å for optimized NR. After edge passivation of the 8a-ZnONR with H atoms (8a-ZnOHC-H), structural deformations inside the NR are not observed as for 8a-ZnONR. For zigzag ZnO nanoribbons (Fig. 1 c, d), we can see that they do not undergo deformation regardless of whether the NR is bare or H-passivated, but retain its original shape.

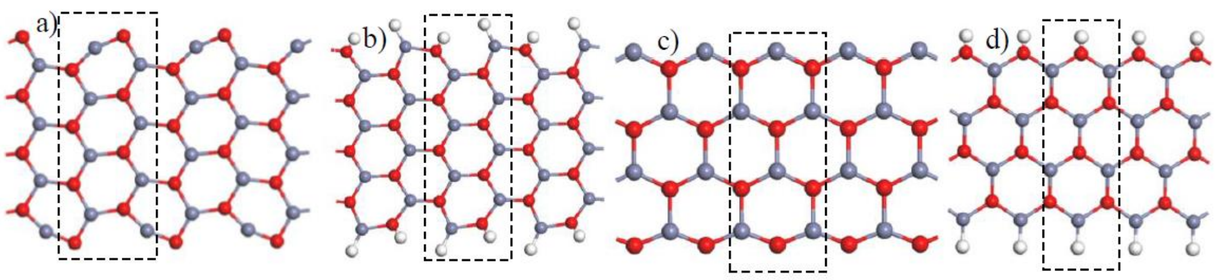

Fig. 1. The optimized structure of ZnO nanoribbons: 8a-ZnONR (a, b) and 8z-ZnONR (c, d).

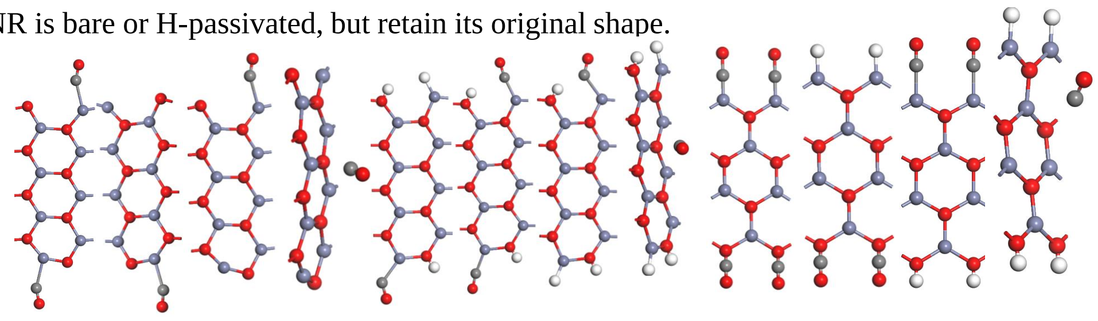

Fig. 2. The optimized structures of CO molecule adsorption in 8a-ZnONR and 8z-ZnONR.

To ensure structural stability, we calculated the binding energy (E_{bin}) for pure and H-passivated ZnO nanoribbons. Analysis obtained results in Table 1 shows that all investigated nanoribbons have a stable structure, which is indicated by the obtained negative values of the binding energy. It should also be noted that the structural stability improves with an increase in the NR width. This tendency is characteristic both for the H absence at the edges of NR and for H-passivated aZnONR-H and zZnONR-H.

Table 1. The binding energy (E_{bin}) and the bandgap (E_g) were calculated for different widths of pure and passivated ZnONRs.

Nanoribbons	E_{bin}, eV	E_g, eV	Nanoribbons	E_{bin}, eV	E_g, eV
6a-ZnONR	−3.44	4.28	6z-ZnONR	−3.87	M
8a-ZnONR	−3.52	4.14	8z-ZnONR	−3.94	M
10a-ZnONR	−3.57	4.08	10z-ZnONR	−3.99	M
6a-ZnONR-H	−3.66	3.82	6z-ZnONR-H	−3.57	0.57
8a-ZnONR-H	−3.68	3.61	8z-ZnONR-H	−3.59	0.34
10a-ZnONR-H	−3.70	3.49	10z-ZnONR-H	−3.60	

Table 2. Calculated adsorption energy for all configurations of adsorption of CO and CO_2 molecules in the ZnONR structure.

Configuration	E_{ad}, eV	Configuration	E_{ad}, eV
CO-8a-ZnONR-CO	−0,77	CO_2-8a-ZnOHC-CO_2	−0,42
CO-8a-ZnONR	−0,45	CO_2-8a-ZnOHC	−0,21
8a-ZnONR-CO	−0,46	8a-ZnOHC-CO_2	−0,21
8a-ZnONR+CO	−0,02	8a-ZnOHC+CO_2	0,02
CO-8a-ZnONR-H-CO	8,71	CO_2-8a-ZnOHC-H-CO_2	8,66
CO-8a-ZnONR-H	−20,70	CO_2-8a-ZnOHC-H	−20,38
H-8a-ZnONR-CO	−20,70	H-8a-ZnOHC-CO_2	−20,57
8a-ZnONR-H+CO	−0,003	8a-ZnOHC-H+CO_2	0,04
CO-8z-ZnONR-CO	3,91	CO_2-8z-ZnOHC-CO_2	4,57
CO-8z-ZnONR-H	−23,91	CO_2-8z-ZnOHC-H	−23,30
H-8z-ZnONR-CO	−25,91	H-8z-ZnOHC-CO_2	−25,55
8z-ZnONR-H+CO	−0,01	8z-ZnOHC-H+CO_2	−0,05

Table 3. Calculated adsorption energy for all configurations of adsorption of NO and NO_2 molecules in the ZnONR structure.

Configuration	E_{ad}, eV	Configuration	E_{ad}, eV
NO-8a-ZnONR-NO	−1,21	NO_2-8a-ZnOHC-NO_2	−1,10
NO-8a-ZnONR	−0,66	NO_2-8a-ZnOHC	−0,53
8a-ZnONR-NO	−0,59	8a-ZnOHC-NO_2	−0,54
8a-ZnONR+NO	−0,45	8a-ZnOHC+NO_2	21,49
NO-8a-ZnONR-H-NO	5,41	NO_2-8a-ZnOHC-H-NO_2	2,99
NO-8a-ZnONR-H	−22,34	NO_2-8a-ZnOHC-H	−23,47
H-8a-ZnONR-NO	−22,34	H-8a-ZnOHC-NO_2	−19,44
8a-ZnONR-H+NO	−0,45	8a-ZnOHC-H+NO_2	−0,36
NO-8z-ZnONR-NO	5,40	NO_2-8z-ZnOHC-NO_2	12,98
NO-8z-ZnONR-H	−21,80	NO_2-8z-ZnOHC-H	−24,51
H-8z-ZnONR-NO	−26,90	H-8z-ZnOHC-NO_2	−27,94
8z-ZnONR-H+NO	−0,56	8z-ZnOHC-H+NO_2	−0,46

To study the sensor properties of ZnO nanoribbons with armchair-like and zigzag-like edges, we built models of NRs under adsorption of CO, CO_2, NO, and NO_2 molecules, and considered different configurations of these molecules with ZnONRs. To determine the stability of the structure of adsorbed molecules in NRs, the adsorption energy (E_{ad}) was calculated and presented in Tables 2, and 3. Fig. 2 presents a schematic representation of various adsorption configurations considered in our study using the example of CO adsorption. In general, for each type of nanoribbon, four possible placements of the adsorbed molecule in the structure of the NR were considered: from both edges of the nanoribbon, separately from each edge, and on the surface of the NR.

The E_{ad} value shows that after the adsorption of a CO molecule on 8a-ZnONR, all configurations are thermodynamically stable and the adsorption process is exothermic, while for 8a-ZnONR with H-passivated, only three configurations are thermodynamically stable, and for the configuration CO-8a-ZnONR-H-CO the adsorption has an endothermic character. When CO is adsorbed on 8z-ZnONR, the CO-8z-ZnONR-CO configuration is also the least energetically favorable, and the other three are thermodynamically stable. The analysis of E_{ad} values shows that the most energetically advantageous for the adsorption of CO molecules is the edge placement of CO atoms on the one hand and H-passivation on the other, regardless of whether the nanoribbon with armchair-like or zigzag-like edges (see Table 2).

During the adsorption of the CO_2 on 8a-ZnONR, three configurations are energetically favorable, except for 8a-ZnONR+CO_2, and adsorption on 8a-ZnONR-H, only two configurations corresponding to single-edge adsorption of the CO_2 molecule and the configuration of edge adsorption of the CO_2 become energetically favorable from two sides and adsorption of CO_2 on the surface of the nanoribbon. In the case of adsorption on 8z-ZnONR, we have only one thermodynamically unfavorable placement of the CO_2, which is the adsorption of the molecule from both ends of the NR. As in the case of the adsorption of the CO, the most energetically advantageous for the CO_2 is the adsorption of this molecule on one side of the NR and H-passivation on the other.

When considering the adsorption of the NO on ZnONRs, the most energetically favorable is the adsorption of the NO on one side of the ZnO nanoribbon for both cases of NR with armchair and zigzag (see Table 3). When considering the adsorption of the NO_2 on ZnONR, the situation concerning the thermodynamic stability of the configurations is similar to the case of the adsorption of the CO_2. Three configurations are thermodynamically stable for 8a-ZnONR, except for the adsorption of the NO_2 molecule on the surface of the NR, and for the H-passivated NR with armchair and zigzag edges, the configuration with adsorption of molecules on both sides of the NRs is energetically unfavorable (see Table 3).